NASA TECHNICAL MEMORANDUM

NASA TM X- 74034

NASA TM X- 74034

NOISE REDUCTION EVALUATION OF GRIDS IN A SUPERSONIC AIR STREAM WITH APPLICATION TO SPACE SHUTTLE

By

John M. Seiner, James C. Manning,
Paul Nystrom, and S. Paul Pao

May 1977

NATIONAL AERONAUTICS AND SPACE ADMINISTRATION
LANGLEY RESEARCH CENTER, HAMPTON, VIRGINIA 23665

1. Report No.	2. Government Accession No.	3. Recipient's Catalog No.
NASA TM X-74034		

4. Title and Subtitle	5. Report Date
Noise Reduction Evaluation of Grids in a Supersonic Air Stream With Application to Space Shuttle	May 1977
	6. Performing Organization Code: 2620

7. Author(s)	8. Performing Organization Report No.
John M. Seiner, James C. Manning, Paul Nystrom, and S. Paul Pao	NASA TM X-74034
	10. Work Unit No.

9. Performing Organization Name and Address	11. Contract or Grant No.
NASA Langley Research Center Hampton, Virginia 23665	
	13. Type of Report and Period Covered: Technical Memorandum

12. Sponsoring Agency Name and Address	14. Sponsoring Agency Code
National Aeronautics and Space Administration Washington, DC 20546	

15. Supplementary Notes

16. Abstract

Near field acoustic measurements were obtained for a model supersonic air jet perturbed by a screen. The objective of the test was to determine if a noise reduction potential would exist in the vicinity of the Space Shuttle Vehicle during ground launch when the rocket exhaust flow is perturbed by a grid.

Both 10 and 12 mesh screens were utilized for this experiment, and each exhibited a noise reduction only at very low frequencies in the near field forward arc. A power spectrum analysis revealed that a modest reduction of from 3 to 5 decibels exists below a Strouhal number $S_t = 0.11$. Above $S_t = 0.11$ screen harmonics increased the observed sound pressure level. The favorable noise reductions obtained with screens for $S_t < 0.11$ may be of substantial interest for the Space Shuttle at ground launch.

17. Key Words (Suggested by Author(s)) (STAR category underlined)	18. Distribution Statement
Space Shuttle, Jet Noise, Screens	Unclassified Unlimited

19. Security Classif. (of this report)	20. Security Classif. (of this page)	21. No. of Pages	22. Price*
Unclassified	Unclassified	34	$4.00

*Available from { The National Technical Information Service, Springfield, Virginia 22161

NOISE REDUCTION EVALUATION OF GRIDS IN A SUPERSONIC AIR STREAM WITH APPLICATION TO SPACE SHUTTLE

John M. Seiner, James C. Manning,
Paul Nystrom*, and S. Paul Pao

SUMMARY

The objective of this investigation was to determine if a noise reduction potential exists in the vicinity of the Space Shuttle Vehicle during ground launch when the rocket exhaust flow is perturbed by a grid. An unheated Mach 2 supersonic air flow was utilized for this test. The flow was generated from a high pressure acoustically treated supply with a 5.08 cm. exit diameter C-D nozzle. Single wire woven screens for both 10 and 12 square mesh were mounted 2 jet diameters above a 122. cm. x 122. cm. x 2.54 cm. thick model launch pad. The 10 and 12 mesh screens had respective open area ratios of .563 and .436. The model launch pad was positioned at 5, 10, and 20 jet diameters downstream of the nozzle exit. Near field microphone levels were recorded with this arrangement at several angles in the jet's forward arc. Jet pressure ratios were selected to generate a fully expanded flow.

Both the 10 and 12 mesh screens exhibited noise reduction only at very low frequencies in the near field forward arc. A power spectrum analysis revealed that a modest reduction of from 3 to 5 decibels exists below a

---

*Graduate Research Assistant, Mechanical Engineering Department, Old Dominion University, Norfolk, Va.

Strouhal number of $S_t = 0.11$. Systematically the smaller reduction could always be associated with a system configuration with the largest observation angle to the jet axis. Above $S_t = 0.11$ screen harmonics increased the observed sound pressure level. The favorable noise reductions obtained with grids for $S_t < 0.11$ may be of substantial interest for the Space Shuttle at ground launch.

INTRODUCTION

There is concern for the very intense low frequency environmental noise in the vicinity of the payload bay of the Space Shuttle vehicle during the liftoff phase of ground launch. These noise components increase in level as the vehicle rises above the launch pad and the rocket engine exhausts are diverted away from the turning buckets and impinge on the exposed surface of the launcher. Very high noise levels exist only during the first few seconds of liftoff and occur at low frequencies which are difficult to attenuate by means of the flight vehicle structure. There is thus a strong motivation to devise some launch pad modifications which would be effective in reducing low frequency noise during liftoff and would not penalize the vehicle during the remainder of the operation. The use of a grid located transverse to the jet exhaust has been suggested as a useful device which could interact with the jet stream and would be easily refurbished after the launch.

In general, solutions that effect a jet noise reduction with a good economy have in the past been difficult to achieve. Over the years many

suppressor configurations have been investigated, and of these, one of the earliest attempts was with the screen perturbed jet. Lassiter and Hubbard (ref. 1) analyzed the effect produced by a 32 mesh screen on the far field noise spectrum and directivity of a model subsonic air jet. They found, dependent upon the screen's location in the jet stream, a low frequency noise reduction of the order of 20 decibels in the direction of maximum radiation. Callaghan and Coles (ref. 2) obtained similar results using a full scale subsonic axial-flow jet engine. Unlike the study of Lassiter and Hubbard they investigated a spectrum of screens with characteristic mesh and open area ratios ranging respectively from 0.5 to 4.0 and .559 to .766. In addition, their far field measurements also included a forward arc survey, which encompasses the radiation direction of interest in the present investigation.

The forward arc results reported by Callaghan and Coles consistently demonstrated an increase in noise level when any one of their screens was inserted into the jet stream. In terms of the total sound power emitted by the screen perturbed jet, only a modest noise reduction could be achieved with screens positioned within 2.5 jet diameters of the nozzle exit. The maximum overall acoustic power level reduction was of the order of 4 decibels.

More recently Arndt, Tram, and Barefoot (ref. 3) considered the effect of a screen on the turbulent structure of a low Mach number, high Reynolds number model air jet. Their objective was to determine how well the scaling

laws of Lilley (ref. 4) could be applied to the screen perturbed jet to predict the observed low frequency and acoustic power reduction. Their turbulence measurements were processed through Lilley's empirical relation, and they obtained good agreement with far field acoustic measurements.

The low frequency reduction in acoustic level is essentially associated with a reduction in the turbulence scale and degree of an isotropic structure. This effect is related to the relief in absolute magnitude of the shear gradient, which results from the fluid momentum loss through the screen. The reduction in shear gradient is responsible for the noise reduction observed in the principle direction of radiation in the jet's far field rear arc. The increased acoustic radiation in the jet's far field forward arc is affiliated with the flow's tendency toward isotropy. The fact that a screen perturbed jet attains a maximum noise reduction for screens positioned relatively close to the nozzle exit can be accredited to the distribution of sound sources in a jet. The research of Laufer, Schlinker, and Kaplan (ref. 5) is of interest for they experimentally measured this distribution for a model supersonic air jet. They found that the peak acoustic source power occurs between 10 and 20 jet diameters.

The studies in references 1, 2, and 3 involved the use of subsonic jets. At the inception of this study it was not clear how a grid would perform in a supersonic stream, and in particular, to what extent the near field forward arc acoustic levels would parallel the far field acoustic results of Callaghan and Coles.

The objective of this study is to investigate if the insertion of a grid transverse to the rocket flow at some point above the launch pad would reduce the amplitude of the radiated noise from the pad into the direction of the Space Shuttle vehicle. The results reported herein describe the extent of the near field noise reduction attainable through use of a 10 and 12 mesh screen located transversely to a supersonic jet stream. These results are presented in terms of overall sound power levels and power spectra for several low passed frequency bands. This information is correlated for both screens for several near field radiation directions as a function of screen axial location and distance to a model launch platform.

EXPERIMENTAL APPARATUS AND PROCEDURE

The experiment was performed using the Supersonic Jet Noise Apparatus at the NASA Langley Research Center. This system is supplied with unheated dry high pressure filtered air, and is throttled by a 3.6 kg./sec. quiet flow valve. The flow is expanded through a Mach 2 C-D nozzle with an exit diameter of 5.08 cm. The regulated flow at the nozzle entrance was acoustically isolated from the valve by three 1.22 meter diameter fiberglass lined mufflers. The resulting 576 to 1 area contraction ratio, in conjunction with the selected nozzle contour, provided a low turbulence and relatively shock free nozzle exit flow as shown in the spark shadowgraph of figure 1. All of the experimental data contained in this report were obtained with the

shock free flow field exhibited in figure 1, which occurred at a pressure ratio of 7.13. The corresponding isentropic jet exit velocity for this pressure ratio was 506 m/sec. The shock free condition was selected for this study, since in the presence of shocks the observed noise reductions could very well depend upon the specific details of the particular shock structure of the model supersonic air jet.

Figure 2 displays a scale model of the Space Shuttle vehicle mounted above the Mobile Launcher platform with attached fuel tank and solid rocket boosters. Several seconds after liftoff, the solid rocket booster shown to the right, is positioned over and above a solid portion of the Mobile Launcher platform.

The Supersonic Jet Noise Apparatus was modified, as shown in figure 3, to simulate the pertinent parameters of the rocket exhaust noise impingement problem. A 122 cm. x 122 cm. x 2.54 cm. thick solid aluminum plate served as a model launch pad. This plate was supported at its center in a manner that provided the opportunity to position the launch pad over a range of several nozzle diameters. For this investigation the range of interest was between 5 and 20 jet nozzle diameters. The rear side of the model launch pad was treated with a damping compound to minimize the plate's low frequency resonant responses.

Two stainless steel 10 and 12 square mesh (number of wires per inch) wire woven screens were utilized in this investigation. Aside from strength, these screens were selected on the basis that their characteristic wire

diameter and open area ratio would scale to a practical configuration of a grid in the Space Shuttle launch arrangement. The 10 and 12 mesh screens had respective open area ratios of 0.563 and 0.436, and were constructed of wire with respective diameters of 0.64 mm and 0.71 mm. For square mesh screens of mesh M and diameter D, the open area ratio β can be calculated from the simple formula $\beta = (1 - MD)^2$.

Each screen was swaged and uniformly tensioned by a ring assembly as shown in figure 3. The ring has an interior diameter of 0.46 m, and was fastened to the launch pad by struts which permitted each screen to be located at 1 and 2 nozzle diameters above the launch pad. These distances were selected on the basis of rocket nozzle clearance that would be required by the full scale prototype.

Four 6.35 mm diameter pressure microphones were used for the near field pressure survey. They were positioned as shown in figure 4, and their coordinates with respect to the nozzle exit are tabulated in table 1. As indicated in table 1, the position of microphone 2 could be varied to study the angular dependence of the rear arc near field pressure. In this sense the data obtained with microphone 2 are of major interest in this study, since it was located close to where the center of the cargo bay doors would be in the Space Shuttle configuration (i.e., $R/D = 6.5$, $\alpha = 152^{o}$). However, due to the geometrical configuration of the supersonic jet, microphone 2 could not be located beyond $\alpha = 145^{o}$ due to a strong acoustic resonance that existed along the nozzle wall.

All four microphones were calibrated before and after each change in model configuration by means of a pistonphone calibrator. This method provides a relative accuracy of ±0.1 decibel between the microphone sensors and permits detection of the absolute level to within 1.0 decibel.

The near field pressure data were conditioned and recorded FM on wide-band magnetic tape at 120 ips (DC - 80 KHz). This was necessary for the fluctuating dynamic pressure drop across a screen was sufficient to eventually shear each screen from its clamp ring. The recorded data were then processed by a real time analyzer for the sound power spectrum as a function of all geometrical parameters under study for this test. A block diagram of the electronic instrumentation used during this test is shown in figure 5.

The chronological order for data acquisition was as follows. First, free jet data (i.e., launch pad located at infinity) were obtained with microphone 2 positioned at $\alpha = 131^{o}$ and 157^{o}. Then the launch pad with and without a screen was tested at 5, 10, and 20 jet diameters with microphone 2 at $\alpha = 121^{o}$, 131^{o}, and 145^{o}. The 10 mesh screen was tested at launch pad distances of 10 and 20 jet diameters only, and for a screen to pad distance of 2 jet diameters. The 12 mesh screen was tested at all three launch pad distances, and with screen to pad distances of 1 and 2 jet diameters. However, the launch pad distance of 5 jet diameters only involved measurement with microphone 2 positioned at $\alpha = 145^{o}$.

At each test location the near field pressure was recorded for all four microphones, and later analyzed in the low pass band levels of 1.1, 6.0, and

80 KHz for the RMS amplitude and pressure spectrum. The pressure spectra reported have not been corrected to the spectrum level, but the filter bandwidth is recorded on each spectrum.

RESULTS AND DISCUSSION

It is important to bear in mind that the results of this study only represent the near field conditions obtained with a model supersonic jet configured as shown in figure 3. The full scale Space Shuttle launch configuration is, of course, much more complex. While the subsonic jet noise problem has been analyzed with fair success, less is known about supersonic jets and rocket exhaust flows. Both the elevated temperature and velocity, coupled with externally reacting gas products and two phase flow, represent significant differences in comparison to the model supersonic flow under consideration. However, the most significant difference between the model shown in figure 3, and the full scale version, is that of geometrical configuration as exemplified by the effects of near field sound scattering. These differences, along with the additional complications introduced by flow screen interaction and flow impingement on the launch pad, preclude an analysis at this time particularly in view of the results which are presented below. Instead we offer the data obtained during this study for what it may be worth in an organized fashion, keeping in mind that the screen-launch pad configuration is a good scale representative.

The pressure spectra reported are presented in terms of both frequency and Strouhal number. In this way the exhaust diameter ratio of 66 to 1, and the velocity ratio of 4.85 is more adequately represented. The Strouhal number S_t is formed by the relation $S_t = fd/v_j$, where in this report f is the observed frequency, D the nozzle exit diameter, and v_j the nozzle exit velocity. The nozzle exit diameter of the model is 5.08 cm., and the nozzle exit velocity is 506 m/sec (exit Mach No. = 1.94). In this study, the Strouhal number range of interest is $S_t \leq 0.139$, which corresponds to a frequency range $f \leq 100$ Hz in the full scale version. For the scale model tests, the corresponding frequency range is $f \leq 1.36$ KHz.

Only the acoustic measurements for microphone 2 are presented at this time. While the data associated with the other three microphones essentially supports the findings discussed below for microphone 2, they do not offer any additional understanding.

RESULTS WITH NOZZLE 10 D ABOVE LAUNCH PAD

These results are presented first, since they fall in line with the chronological order of the test, and they represent the region of highest density in parameter variation. In almost all cases observed, the insertion of either one of the screens in the supersonic flow produced higher overall noise levels in the radiation direction of interest. Figure 6 illustrates the general overall performance of both the 10 and 12 mesh screens submerged

transverse to the flow at 2 D above the launch pad surface. The spectra are presented in contrast to the spectra observed with the free jet and launch pad without screen. Even though the launch pad screen configuration introduces considerably high pressure fluctuations, the spectral shape for $S_t > 1$ appears preserved, suggesting a uniform broadband increase in noise by either screen. The useful frequency range of these spectra is limited to 80 KHz by the tape recorder frequency response.

For Strouhal number's $S_t < 1$ each screen generates strong harmonics primarily in the frequency range $0.3 < S_t < 0.5$. These characteristics are better illustrated by figure 7, which displays the same information for microphone 2 processed in a 10 KHz band. As can be observed in figure 7, the strong harmonics associated with each screen occur at different spectral locations. Since both screens were located 2 D above the launch pad surface, the spectral locations are more than likely associated with a screen characteristic. Figure 8, which compares the 12 mesh screen at 1 D and 2 D above the launch pad surface, demonstrates that the amplitude of these harmonics is strongly related to the distance of the screen above the launch pad.

It is difficult to establish a relation that identifies just what screen characteristic is associated with the spectral peaks of figure 7. At first, the time scale associated with these peaks may appear to be associated with a global screen scale in the order of one jet diameter. However, the more obvious choice of pore size ℓ can be related to these peaks by assuming a normal shock across the screen face impacted by the supersonic flow and

application of the resistance formula for screens offered by Wieghardt (ref. 6). The normal shock relations are used to calculate an incident characteristic flow velocity, and Weighardt's results are used to calculate the pressure drop or downstream characteristic velocity u*. Thus, if one assumes that a series of cell like jets emerge from the screen with a characteristic time scale of ℓ^*/u^*, then for the 3.8 KHz peak of the 12 mesh screen in figure 7, we have that $\ell^* = 0.69\ \ell$. For subsonic circular jets the axial turbulence integral length scale is approximately D/2 in the region of maximum noise production. Therefore, the pore size ℓ of the screen may serve as an equivalent parameter in the screen configuration. Similarly the 10 mesh screen's peak of 3.1 KHz in figure 6 produces a characteristic length scale $\ell^* = 0.59\ \ell$, which is consistent with the above results for the 12 mesh screen. This calculation suggests that a nonuniform grid may improve the reduction obtained here with a uniform grid.

While both figure 7 and 8 indicate that either screen produces undesirable harmonics, they occur at frequencies above the reduced frequency $S_t = .139$ (i.e., f > 100 Hz in full scale model). In figures 9, 10, and 11 the results for the 10 and 12 mesh screens are displayed in the reduced frequency range $S_t = 0 \rightarrow 1.2$ for several angular positions of microphone 2. As can be observed from these figures, the reduction obtained depends on the angle α, the largest occurring with microphone 2 positioned further away from the nozzle wall. For all angles α, however, the largest reduction occurs in the vicinity of $S_t = 0.015$.

In figure 8 it was shown that the 12 mesh screen produced less noise in the 10 KHz band when located closer to the launch pad surface. Even though

these data do indicate that the least noise increase in this band may occur for screens at the surface of the launch pad, figure 12 shows a substantial noise reduction for the 12 mesh screen 1 D above the launch pad in the 1.2 KHz band. Both figures 8 and 12 clearly suggest that the 1 D distance to the launch pad surface and a higher mesh screen are more desirable features.

RESULTS WITH NOZZLE 20 D ABOVE LAUNCH PAD

It is important to point out that in a coordinate system with an origin at the launch pad surface, the fixed microphone 2 positions listed in table 1 actually appear more normal to the plane of the screen with increasing downstream distance. The previous results at 10 D indicated that for directions farther away from the normal of the screen's plane greater noise reductions can be achieved. Thus, for a launch pad distance of 20 D, one should expect to find smaller reductions in the reduced frequency band $0 < S_t < 1.2$. In fact, this is what is found for the 10 mesh screen results shown in figure 13 for the microphone 2 angle of $\alpha = 131^{o}$. As a means for convenient comparison, the 10 mesh results at 10 D have been cross-plotted in figure 13. For the other microphone angles of $\alpha = 121^{o}$ and 145^{o}, the results at 20 D show the same directional trend as the data at 10 D.

RESULTS WITH NOZZLE 5 D ABOVE LAUNCH PAD

The test plan at 5 D did not include measurements of directionality. However, on the basis of the above results for microphone 2 data at $\alpha = 145^{o}$, one should expect even stronger reductions in the reduced frequency band $0 < S_t < 1.2$ at 5 D. Figure 14 demonstrates this consistent trend with

one notable exception. The 12 mesh screen results are more favorable with the screen positioned 2 D above the launch pad surface rather than 1 D. This is in contrast to what was observed with the launch pad at 10 D.

It is also of interest to note the performance of the 12 mesh screen at 5 D in the 10 KHz band. Figure 15 shows that the screen produces less noise in this band compared to the launch pad without screen, and for either the 1 D or 2 D distances. This particularly encouraging result demonstrates the importance of directionality on the observed results.

SUMMARY OF LOW PASS BAND LEVEL AMPLITUDES

In table 2 the measured true root mean square low pass band level reductions in decibels relative to 0.0002 μ bar have been assembled for all test measurements concerned with microphone 2. This table shows that in the 1.1 KHz band the pressure increases with increasing downstream distance for the launch pad without screen. However, as expected, the overall pressure level in the 80 KHz band decreases with increasing downstream distance. It is unfortunate that the reductions obtained with the screens are less effective with increasing downstream distance in the 1.1 KHz band.

A much clearer view of these results can be observed in table 3, which compares the band levels obtained with the screens relative to those with the launch pad without a screen. As can be observed in table 3, the largest reductions in the 1.1 KHz band occur for the shorter launch pad to nozzle distances and at angles less acute to the jet exit nozzle axis. The reductions at 5 D are particularly encouraging when one considers that this

would correspond to frequencies f < 100 Hz in the full scale model. It is clear from table 3 that the best overall performance was obtained with the 12 mesh screen at 1 D above the launch pad surface. For this particular configuration, the screen harmonics in the 6 KHz band were minimal, and at the same time important reductions were obtained in the low pass band of interest.

CONCLUDING REMARKS

The objective of this investigation was to determine from model tests if a noise reduction potential exists in the vicinity of the Space Shuttle vehicle at ground launch when the rocket exhaust flow is perturbed by a grid. The data obtained do indicate that a favorable reduction in the reduced frequency band of interest $S_t < 0.139$ can be attained. The data also indicate that grids having less open area provide greater reductions, although sufficient care is required in locating the screen above the launch pad to minimize strong harmonics introduced by the screen in the range $0.2 < S_t < 0.5$. The data also show that the overall pressure level increases with increasing nozzle exit to launch pad distance in the range 5 to 20 D, and that both 10 and 12 mesh screens are less effective at increasing altitudes. In view of the great aerodynamic and geometrical differences between the full scale version and the model used in the investigation, the results presented must be interpreted with caution.

REFERENCES

1. Lassiter, L. W.; and Hubbard, H. H.: Some Results of Experiments Relating to the Generation of Noise in Jets. J. Acoust. Society America, vol. 27, no. 3, May 1955, pp. 431-437.

2. Callaghan, E. E.; and Coles, W. D.: Investigation of Jet-Engine Noise Reduction by Screens Located Transversely Across the Jet. NACA TN 3452, 1955.

3. Arndt, R. E. A.; Tram, N.; and Barefoot, G.: Turbulence and Acoustic Characteristics of Screen Perturbed Jets. AIAA Paper No. 72-644, June 1972.

4. Lilley, G. M.: On the Noise From Air Jets. Aeronautical Research Council 20, 376, Sept. 1958.

5. Laufer, J.; Schlinker, R.; and Kaplan, R. E.: Experiments on Supersonic Jet Noise. AIAA Paper No. 75-478, March 1975.

6. Wieghardt, K. E. E.: On the Resistance of Screens. The Aeronautical Quarterly, vol. IV, 1953.

TABLE I - MICROPHONE LOCATIONS

Microphone No.	R/D	α
1	2.50	90^{o}
2	1.94	157^{o} †
	2.18	145^{o}
	2.66	131^{o}
	3.42	121^{o}
3*	20.00	90^{o}
4**	10.00	90^{o}

* Located at $\psi = 21^{o}$ in Azmuithal Plane

** Located at $\psi = 135^{o}$ in Azmuithal Plane

† Free Jet Data Only

Table II. Band Level Differences With Respect to No Screen

		LAUNCH PAD WITHOUT SCREEN			LAUNCH PAD AT 5 D		LAUNCH PAD AT 10 D			LAUNCH PAD AT 20 D		LOW PASS FILTER BAND kHz
α DEGREES	FREE JET	5 D	10 D	20 D	12 MESH AT 1 D	12 MESH AT 2 D	12 MESH AT 1 D	12 MESH AT 2 D	10 MESH AT 2 D	12 MESH AT 2 D	10 MESH AT 2 D	
121	*	*	124.4	128.0	*	*	117.8	118.4	119.0	*	126.0	1.1
131	113.3	*	125.1	129.0	*	*	119.5	118.7	119.3	*	126.7	1.1
145	*	122.7	125.1	129.3	116.5	114.2	118.4	120.0	121.4	*	128.6	1.1
157	114.2	*	*	*	*	*	*	*	*	*	*	1.1
121	*	*	138.3	128.8	*	*	139.3	142.9	141.8	*	129.0	6.0
131	126.7	*	138.1	129.2	*	*	139.4	141.2	142.8	*	129.6	6.0
145	*	136.0	137.9	129.8	136.2	133.8	139.8	147.3	144.4	*	129.9	6.0
157	126.1	*	*	*	*	*	*	*	*	*	*	6.0
121	128.4	*	144.4	138.2	*	*	144.6	146.7	146.8	*	139.2	80.0
131	127.3	*	143.1	138.5	*	*	144.3	147.1	147.2	*	139.4	80.0
145	126.3	147.8	142.3	139.0	145.2	146.2	143.8	152.3	148.4	*	139.6	80.0
157	126.2	*	*	*	*	*	*	*	*	*	*	80.0

Table III. Low Pass Filter Band Level Reductions in DB re. 0.0002 Microbar

	LAUNCH PAD AT 5 D		LAUNCH PAD AT 10 D			LAUNCH PAD AT 20 D		LOW PASS FILTER BAND kHz
α DEGREES	12 MESH AT 1 D	12 MESH AT 2 D	12 MESH AT 1 D	12 MESH AT 2 D	10 MESH AT 2 D	12 MESH AT 2 D	10 MESH AT 2 D	
121	*	*	-6.6	-6.0	-5.4	*	-2.0	1.1
131	*	*	-5.6	-6.4	-5.8	*	-2.3	1.1
145	-6.2	-8.5	-6.7	-5.1	-3.7	*	-0.7	1.1
157	*	*	*	*	*	*	*	1.1
121	*	*	+1.0	+4.6	+3.5	*	+0.2	6.0
131	*	*	+1.3	+3.1	+4.7	*	+0.4	6.0
145	+0.2	-2.2	+1.9	+9.4	+6.5	*	+0.1	6.0
157	*	*	*	*	*	*	*	6.0
121	*	*	+0.2	+2.3	+2.4	*	+1.0	80.0
131	*	*	+1.2	+4.0	+4.1	*	+0.9	80.0
145	-2.6	-1.6	+1.5	+10.0	+6.1	*	+0.6	80.0
157	*	*	*	*	*	*	*	80.0

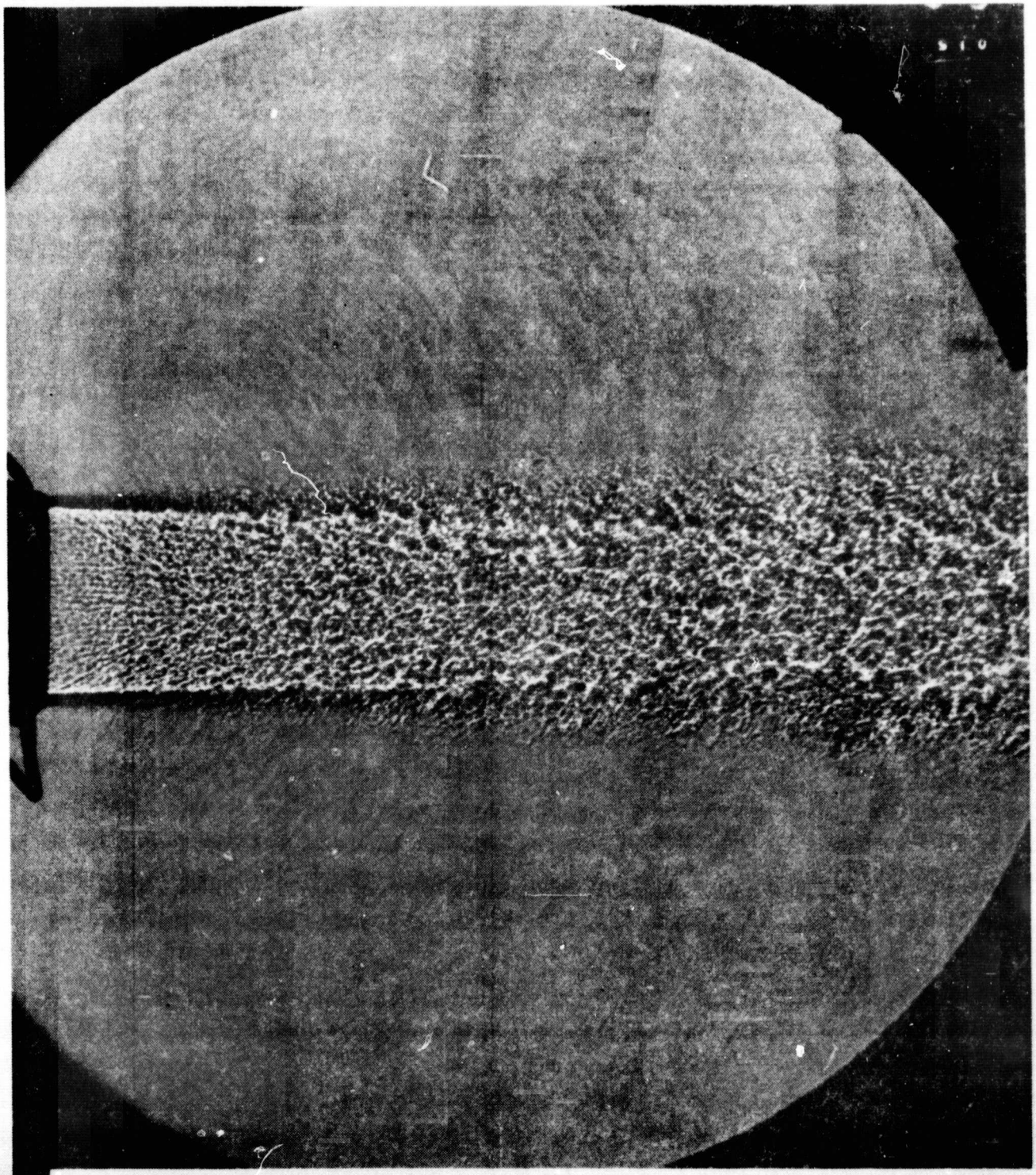

Figure 1. Spark Shadowgraph of Free Jet at a Pressure Ratio of 7.13

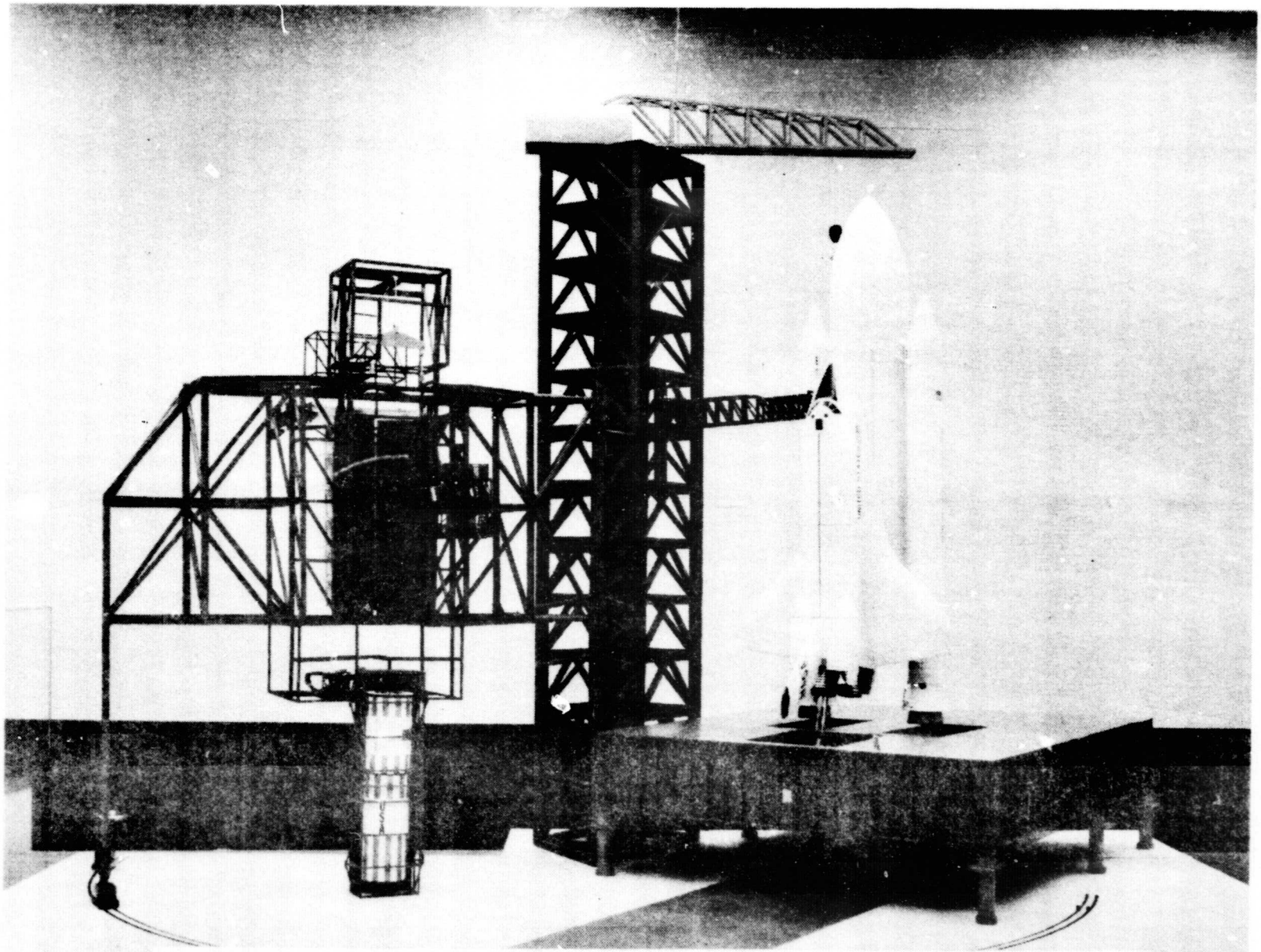

Figure 2. Scale Model of Space Shuttle Mounted Above Mobile Launcher Platform

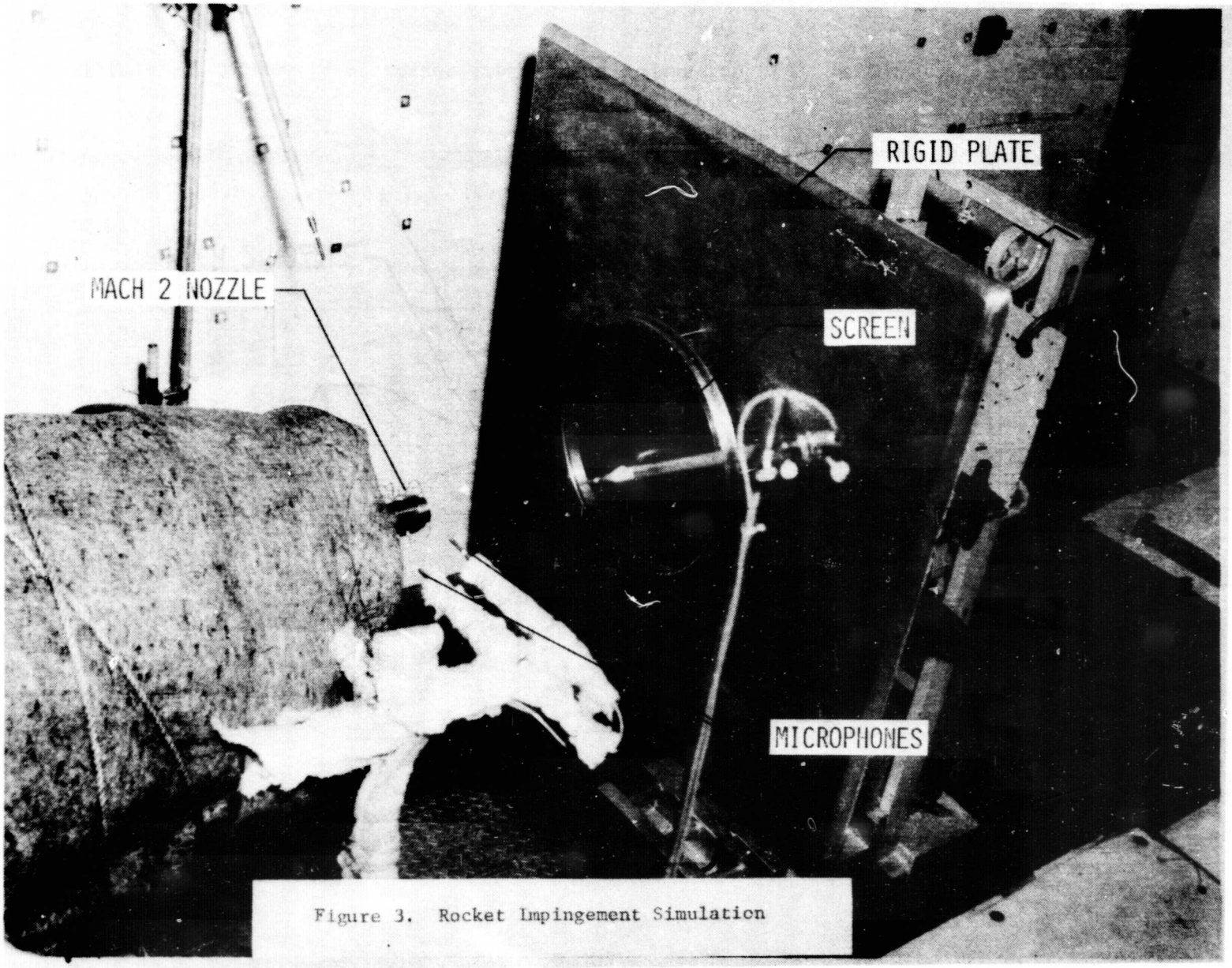

Figure 3. Rocket Impingement Simulation

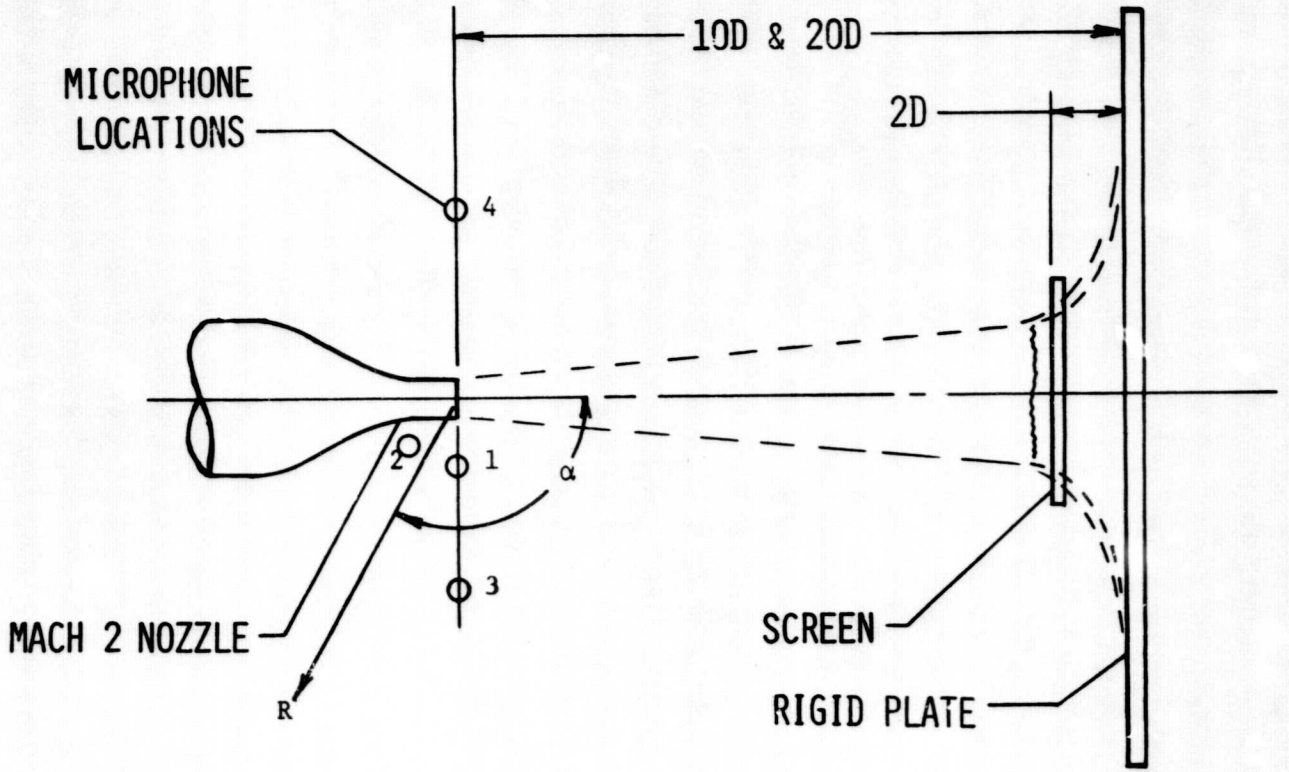

Figure 4. Schematic of Rocket Impingement Simulation

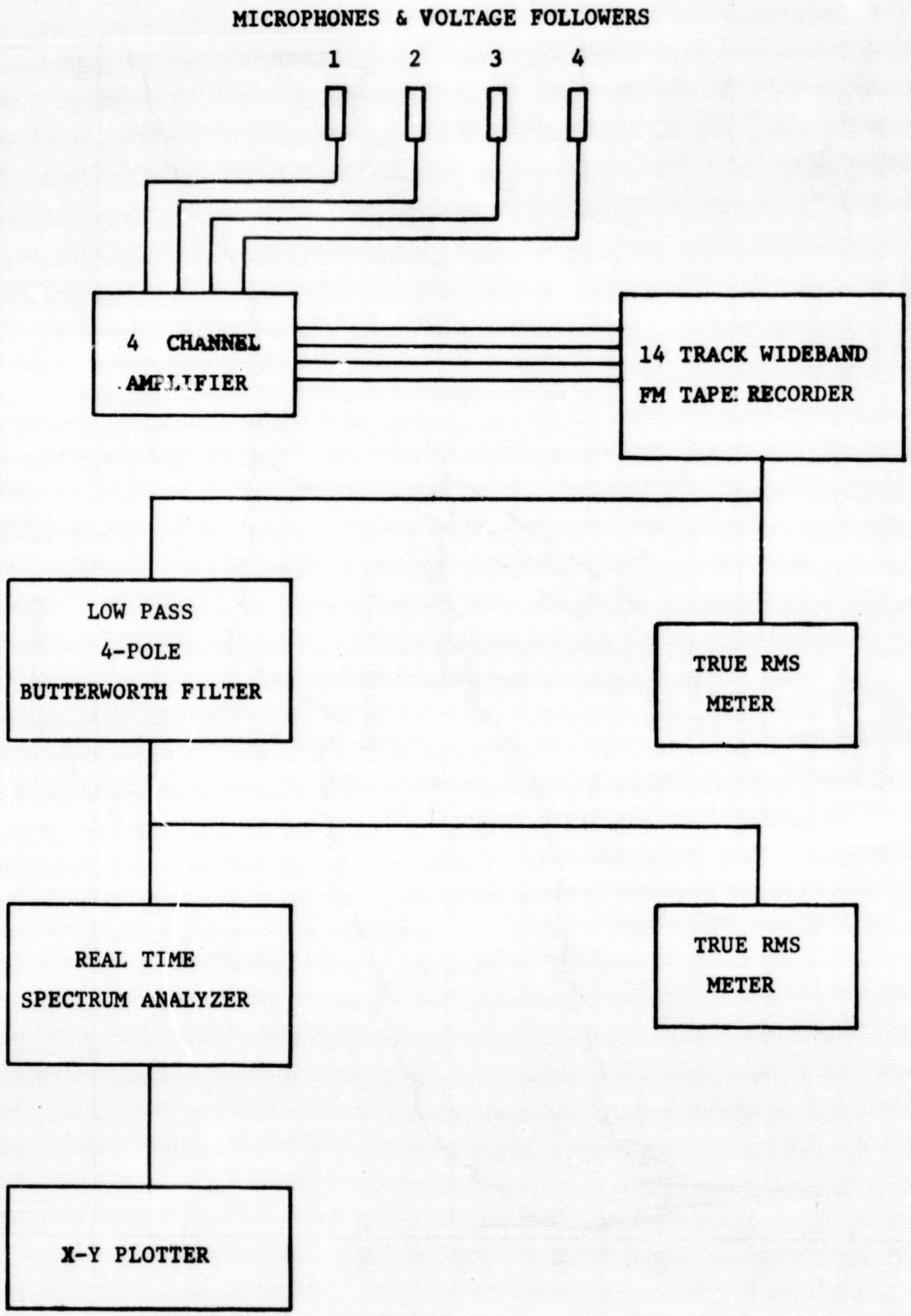

Figure 5. Block Diagram Of Electronic Instrumentation

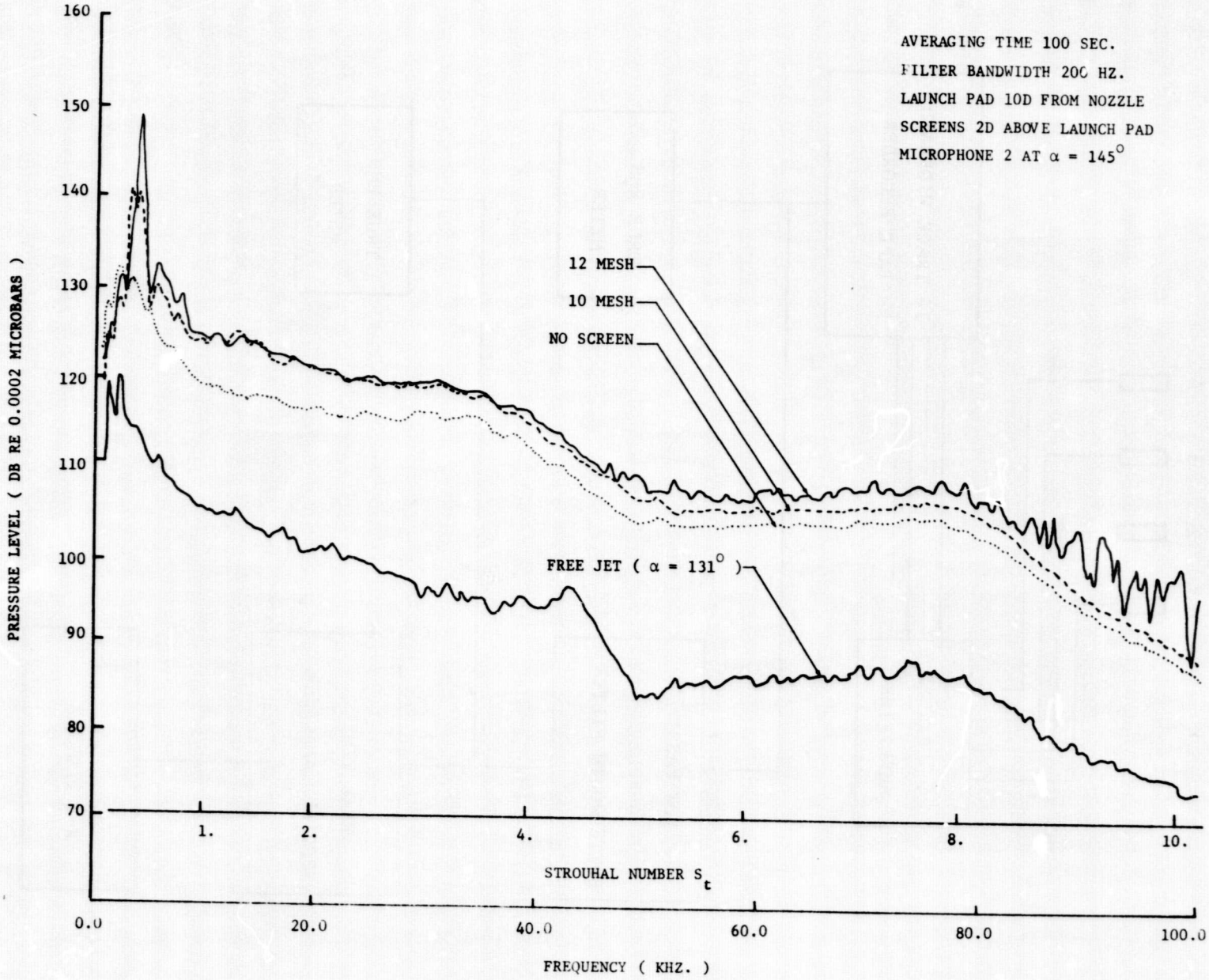

Figure 6. Microphone 2 Pressure Spectra 0,8. S_t for $\alpha = 145^\circ$

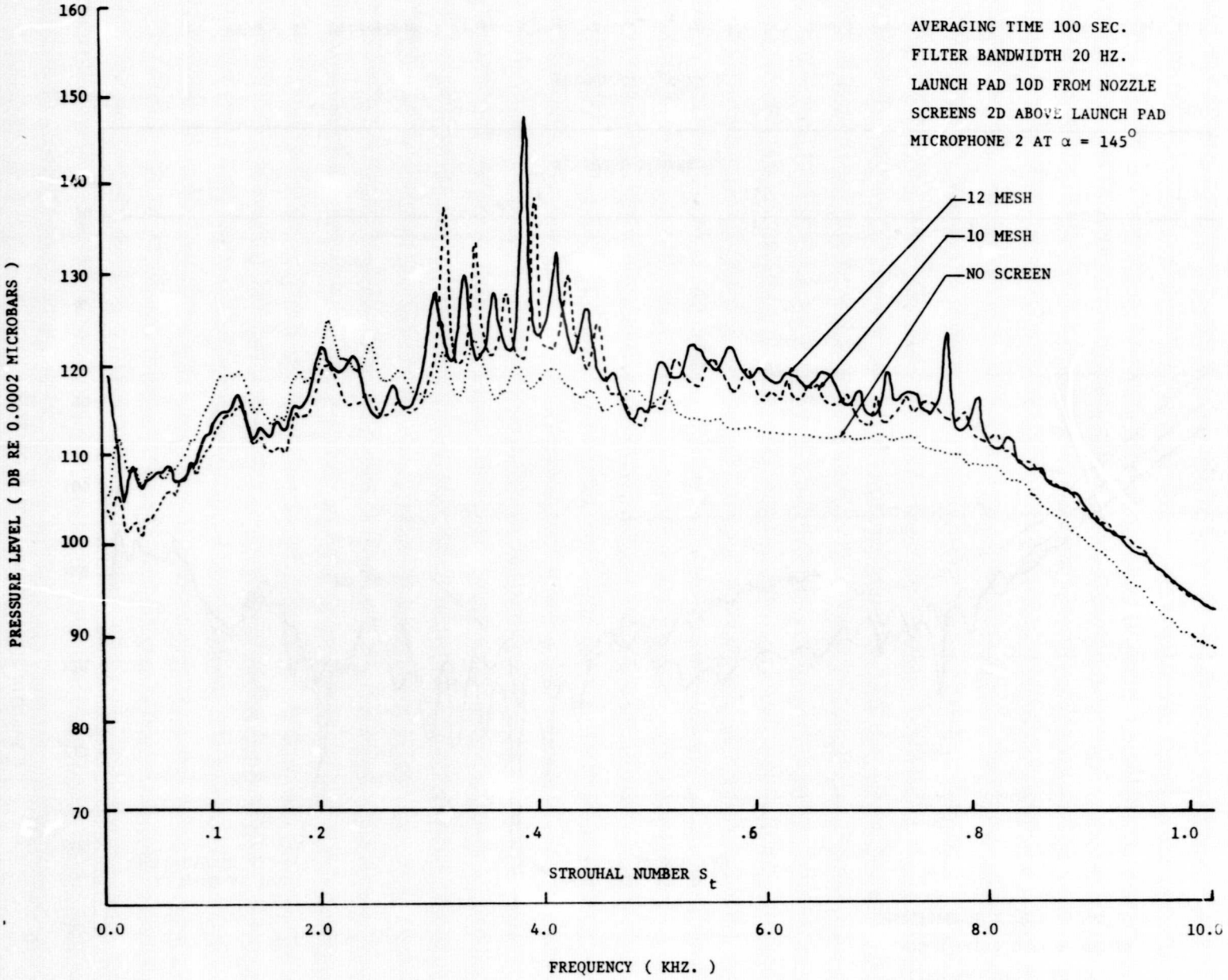

Figure 7. Pressure Spectra 0,1. S_t for $\alpha = 145^\circ$

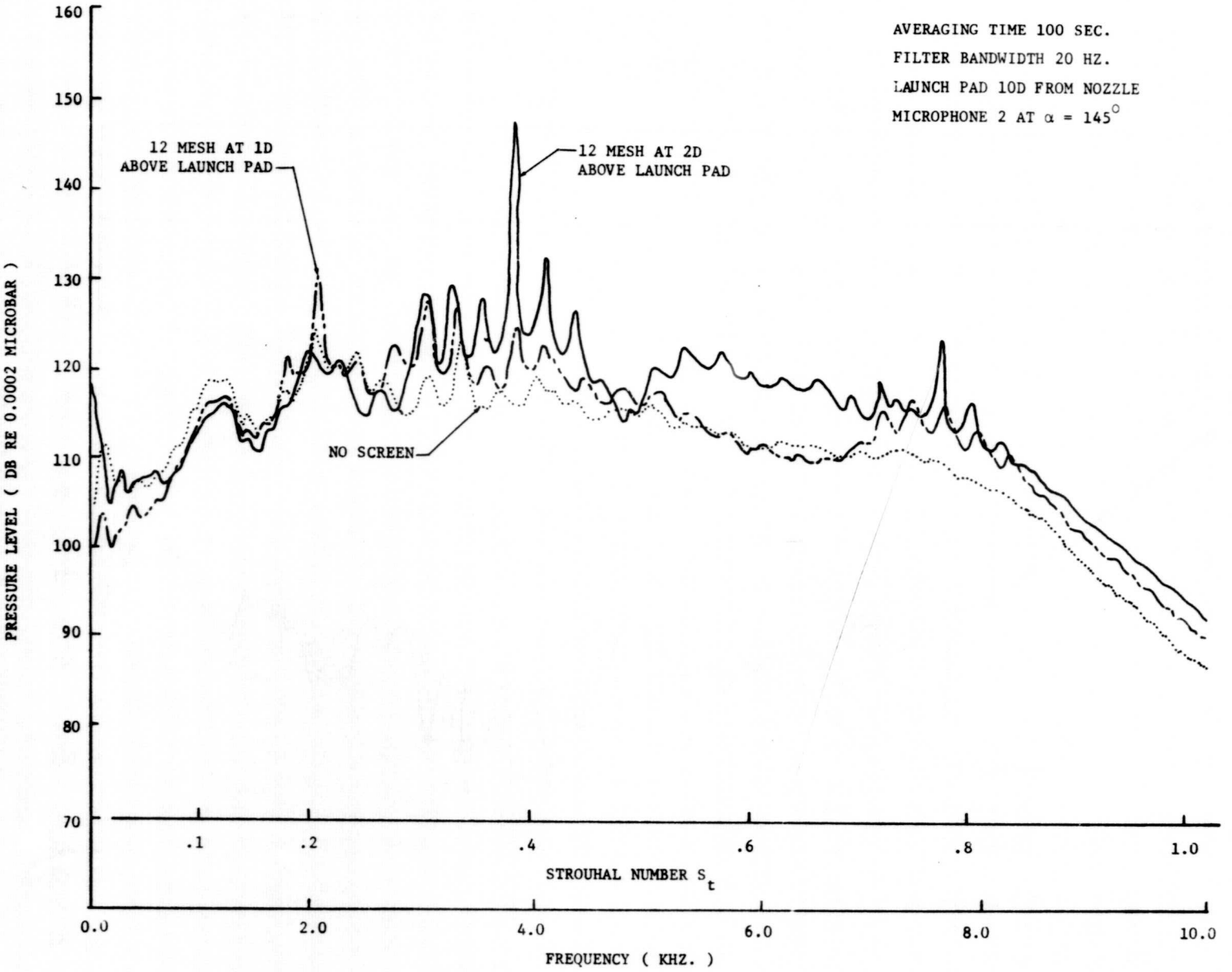

Figure 8. Microphone 2 Pressure Spectra 0,1. S_t for $\alpha = 145^\circ$ and 12 Mesh Screen 1 & 2D Above Launch Pad

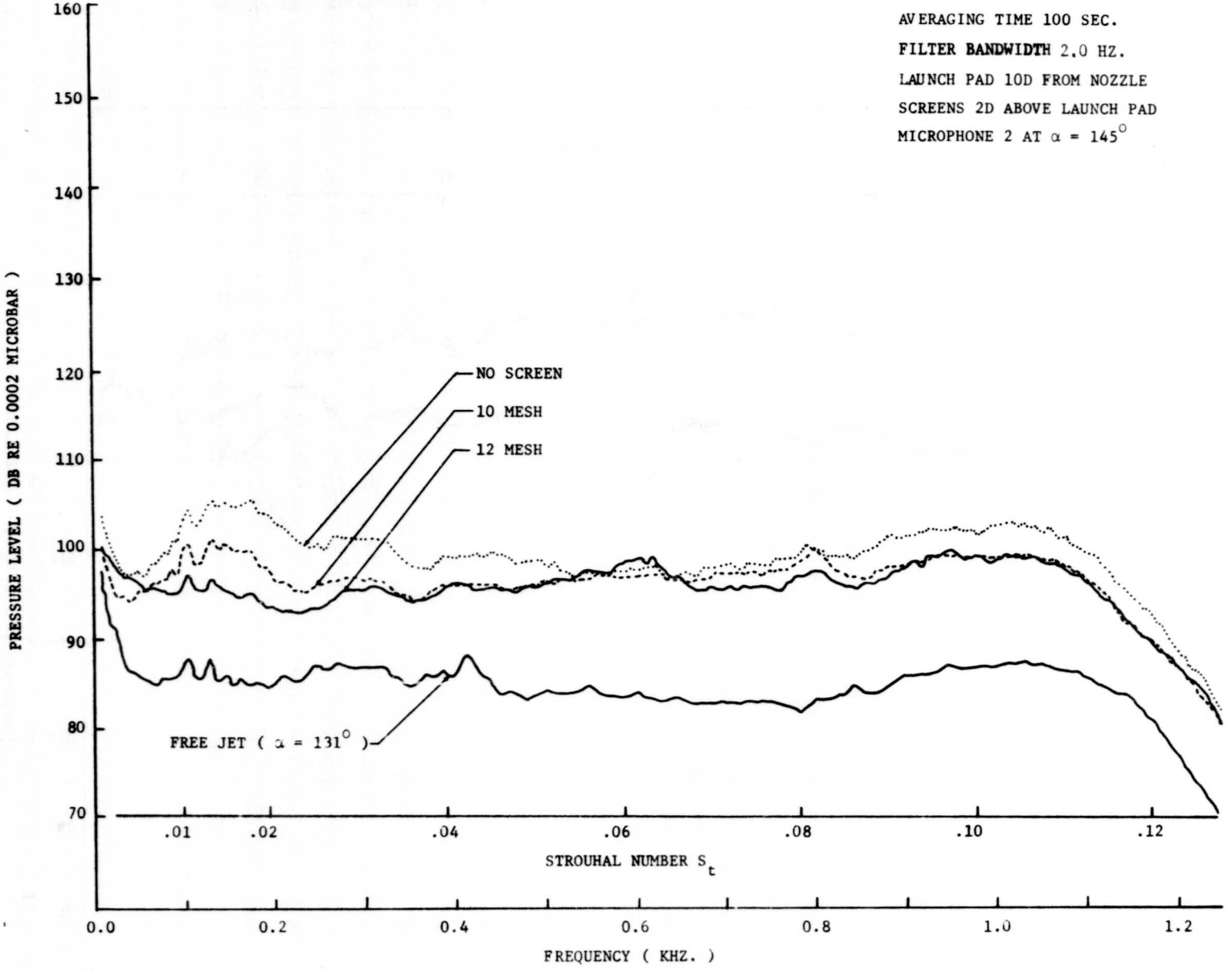

Figure 9. Microphone 2 Pressure Spectra 0,0.12 S_t for $\alpha = 145^{\circ}$

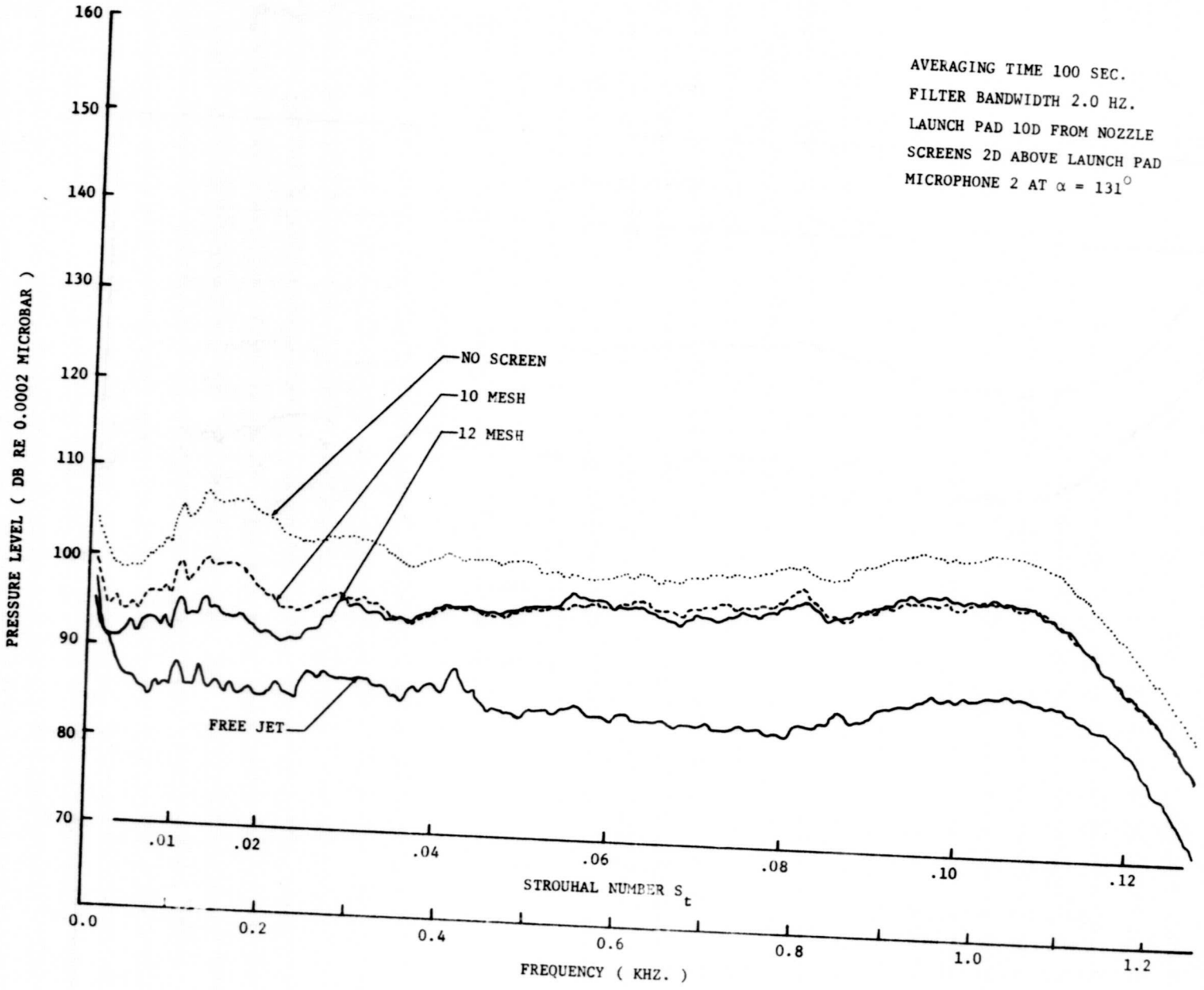

Figure 10. Microphone 2 Pressure Spectra 0,0.12 S_t for $\alpha = 131^{\circ}$

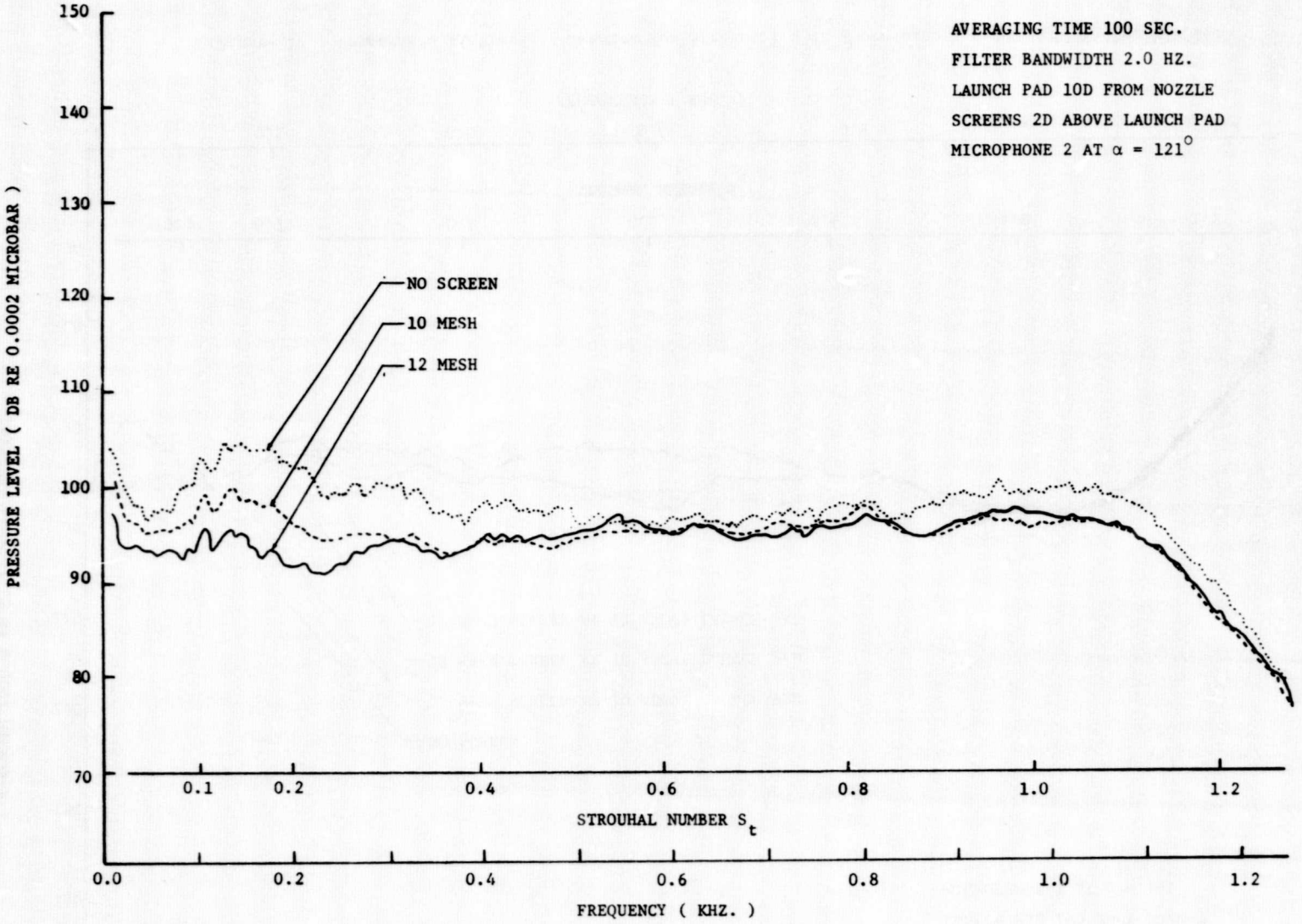

Figure 11. Microphone 2 Pressure Spectra 0,0.12 S_t for $\alpha = 121^\circ$

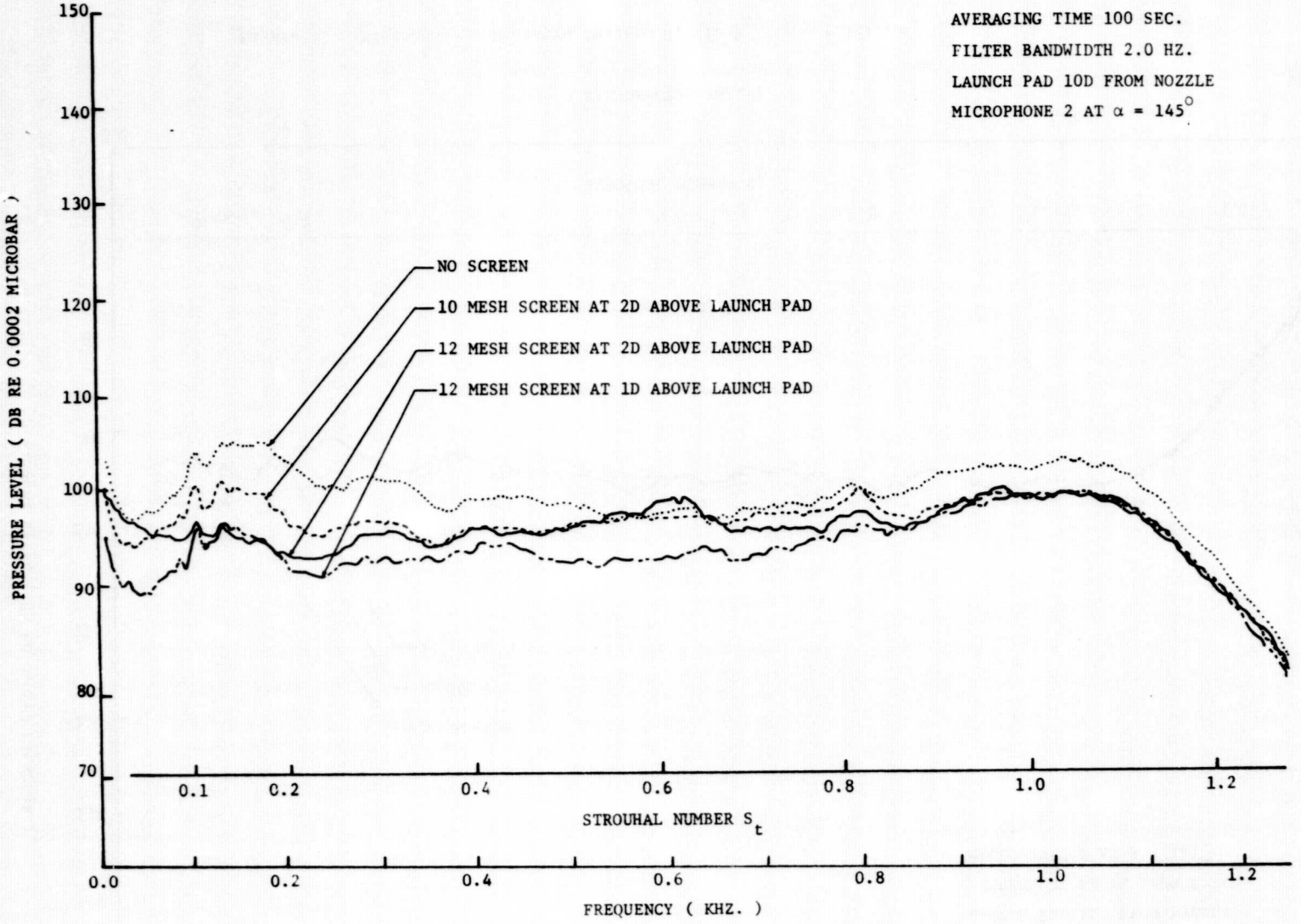

Figure 12. Comparison of Pressure Spectra for Screens 1 & 2D Above Launch Pad 0,0.12 S_t for $\alpha = 145^\circ$

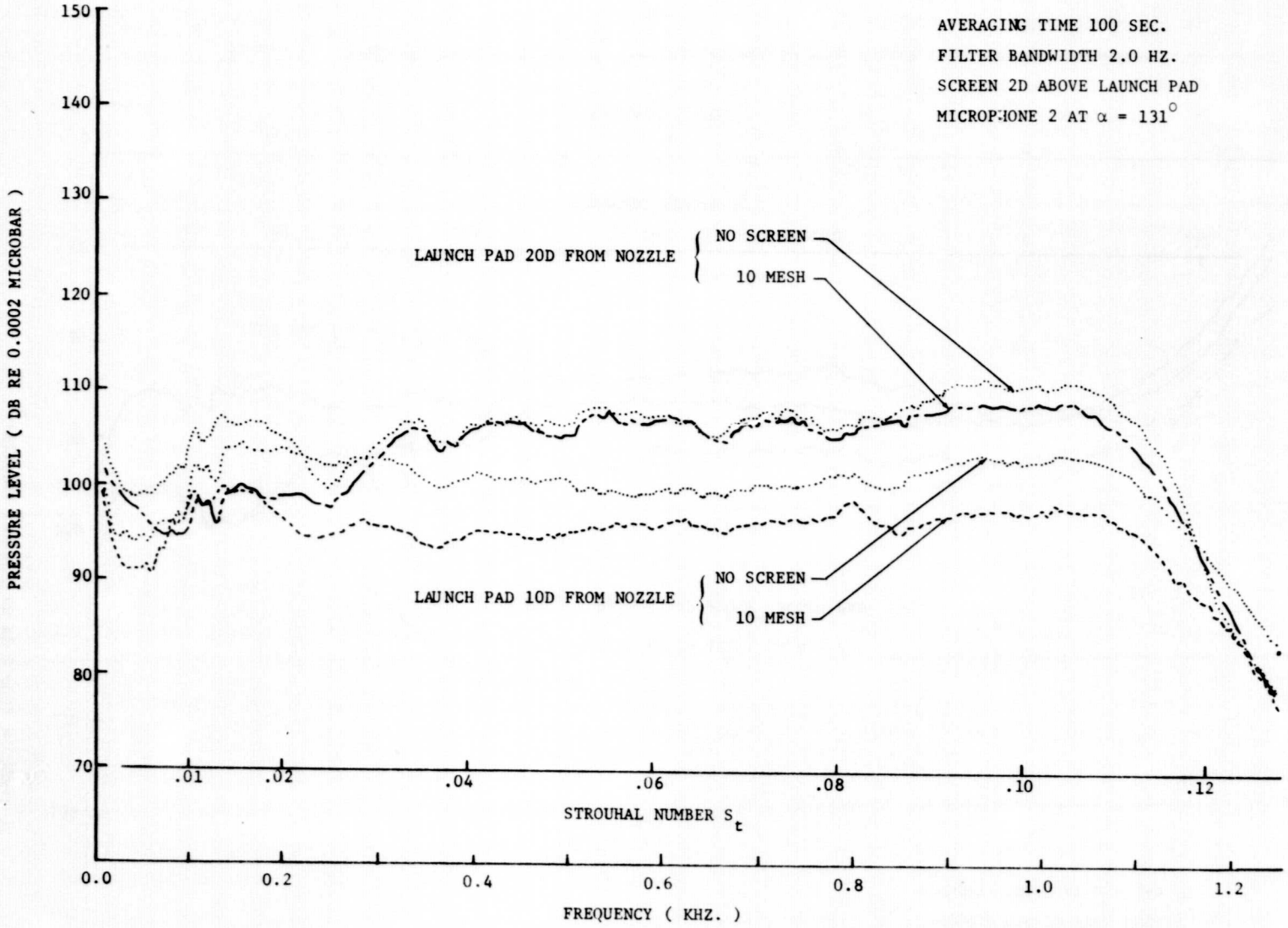

Figure 13. Comparison of Pressure Spectra 0,0.12 S_t for Nozzle Exit at 10 & 20D from Launch Pad

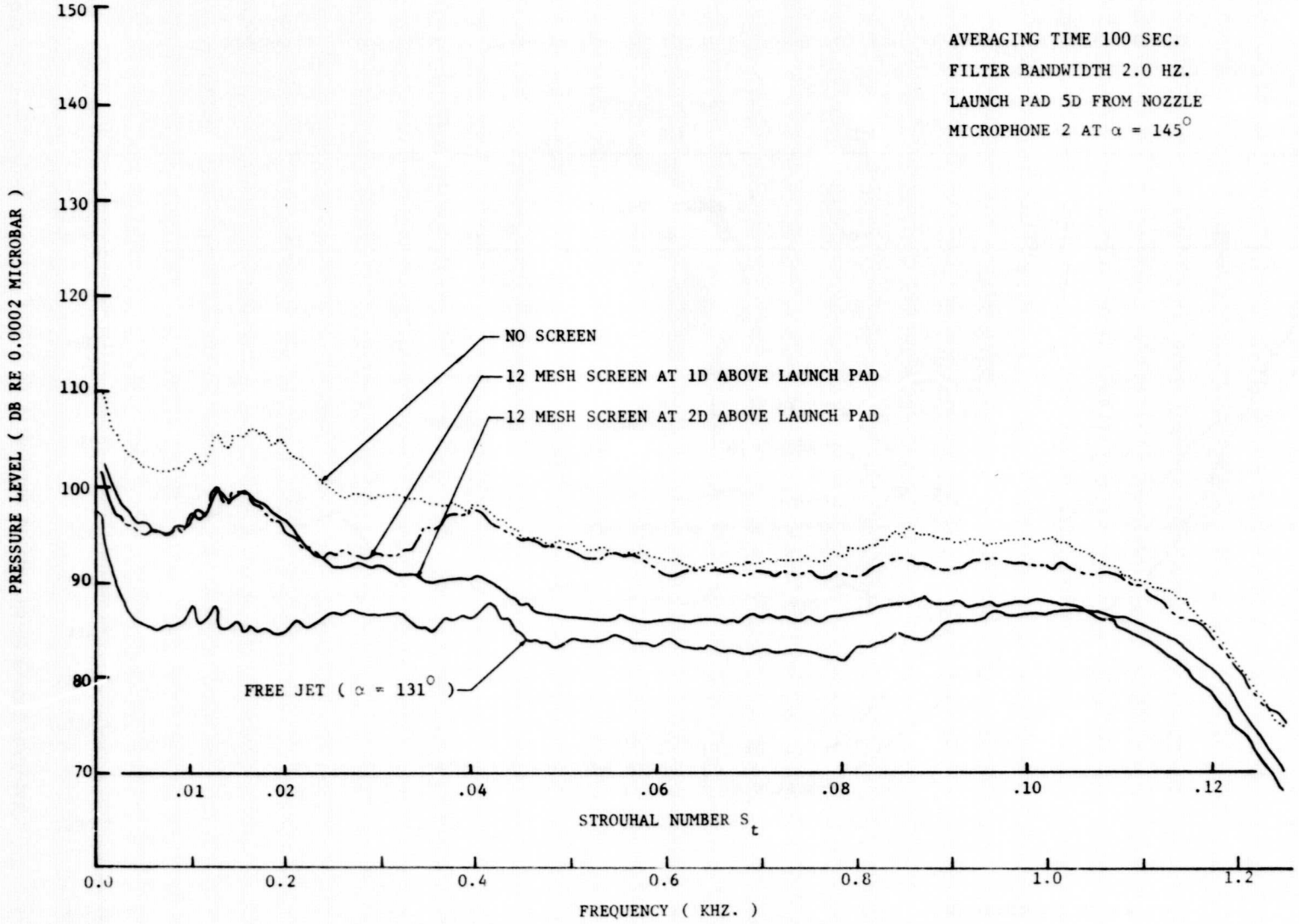

Figure 14. Pressure Spectra 0,0.12 S_t for Nozzle Exit 5D from Launch Pad

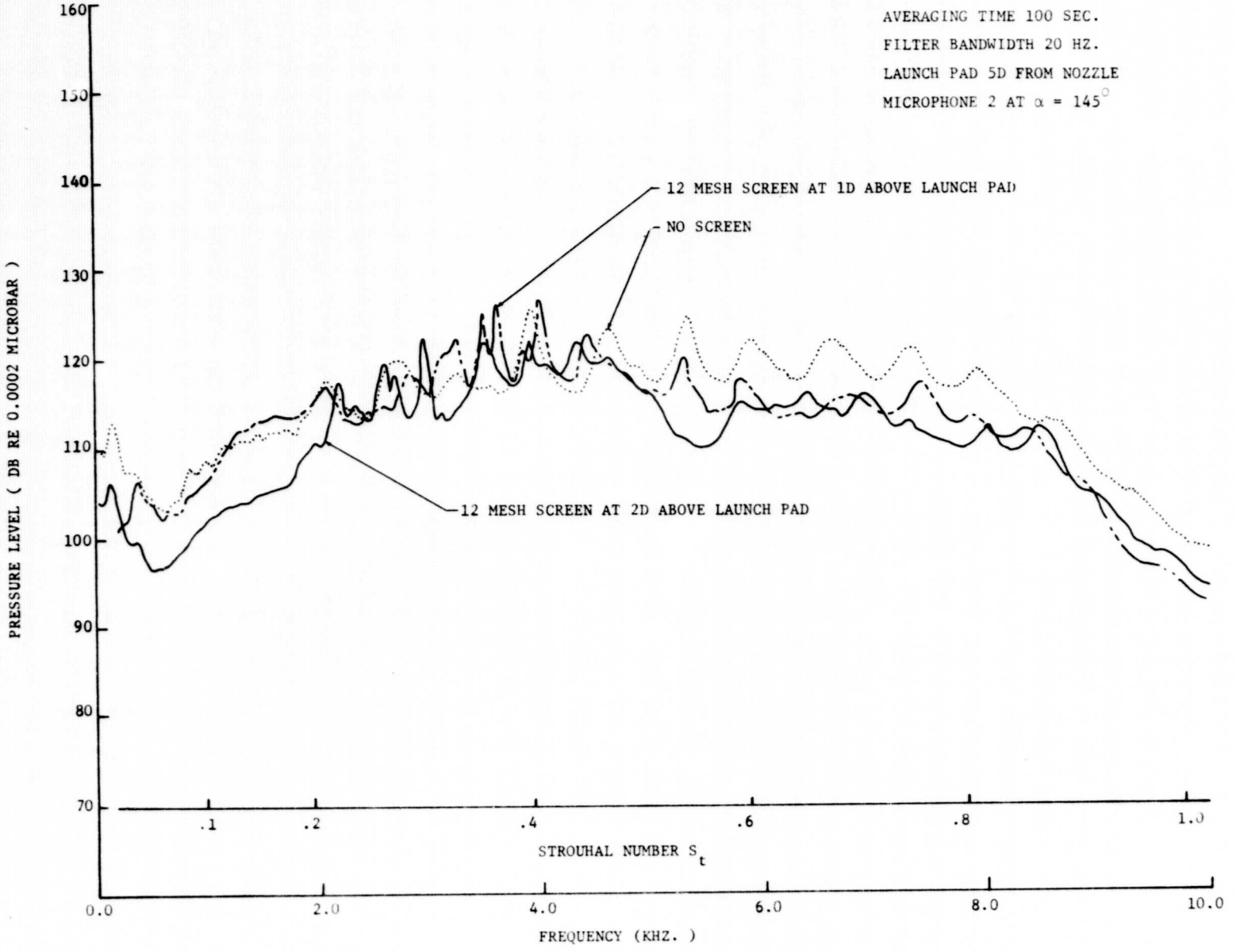

Figure 15. Pressure Spectra 0,1.0 S_t for Nozzle Exit 5D from Launch Pad